Carbon Monoxide Complexes of Iron(II): Synthesis and Structural Studies of Five- and Six-Coordinate Complexes of the Macrocyclic Ligand, $C_{22}H_{22}N_4^{2-}$

Virgil L. Goedken,*[1] Shie-Ming Peng, JoAnn Molin-Norris, and Young-ae Park

Contribution from the Department of Chemistry, The University of Chicago, Chicago, Illinois 60637. *March 1, 1976*

Abstract: Iron(II) complexes of the 7,16-dihydro-6,8,15,17-tetramethyldibenzo[*b,i*][1,4,8,11]tetraazacyclotetradecinato ligand, a [14]annulene ligand, bind carbon monoxide very strongly as indicated from iron carbonyl stretching frequencies in the range 1940–1915 cm^{-1}. A five-coordinate carbon monoxide complex having no trans ligand and six-coordinate complexes having amine axial ligands have been isolated and characterized. X-ray crystal structures of three complexes, the five-coordinate complex, $[Fe(C_{22}H_{22}N_4)(CO)]\cdot\frac{1}{2}C_7H_8$, and six-coordinate complexes having pyridine and hydrazine as axial ligands have been determined.The Fe–CO bond is linear an appears normal in all the structures. The ligands trans to the CO have abnormally long Fe–N distances, 2.088 (3) and 2.122 (5) Å for the pyridine and hydrazine complexes, respectively. The Fe(II) atom is displaced significantly, 0.29 and 0.11 Å, from the N_4 donor plane in the five-coordinate complex and the six-coordinate hydrazine complex, respectively. The displacement is attributed to the combined effects of strong Fe–CO binding and steric interactions within the macrocyclic ligand. The average Fe–N_4 distance, 1.94 Å, for the three structures is significantly shorter than observed in low-spin Fe(II) porphyrin structures. Double bond delocalization of the macrocyclic ligand is limited to the 2,4-pentanediiminato chelate rings and to the benzenoid rings.

In recent years, the study of iron–porphyrin and related macrocyclic complexes has intensified. The objectives have been twofold. One has been the better understanding of the fundamental chemistry associated with iron in various strong-field planar-ligand environments and having a variety of axial interactions. The other is the synthesis and study of compounds which isolate or emphasize essential features of naturally occurring heme complexes. In this regard, much effort has focused on the synthesis and study of complexes capable of reversibly coordinating molecular oxygen. Much of the mystique associated with the binding of molecular oxygen by natural occurring hemes has been removed by the highly successful challenge to this problem by a number of investigators employing a variety of strategies.[2–4]

The well-known toxicity of carbon monoxide to life is largely due to the stronger binding of CO, by a factor of 200, over molecular oxygen by many of the heme complexes. The CO binding constants of the native heme proteins, hemoglobin, myoglobin, and cytochrome P450, are extremely high and on the order of 10^8.[5] The factors governing the stability of carbon monoxide binding, while simple in principle to evaluate, are difficult in practice to assess with a high degree of reliability. In general, ligand features contributing to the radial expansion of the d_π orbitals and facilitating $_\pi$(Fe)–π^*(CO) back-bonding are predicted to lead to strong Fe–CO bonds. The sensitivity of Fe(II)–CO binding constants to minor changes of ligand environment can be best illustrated with a few examples. Consider first the Fe(II) heme complexes. The binding constants for native hemoglobin and myoglobin are on the order of 10^8,[6] but those of isolated iron(II) heme complexes are much lower, on the order of 10^4.[7] Although phthalocyanine ligands have strong structural similarities to porphyrins, iron(II) phthalocyanine complexes have exceedingly low affinities for CO with binding constants of approximately 10^{-2}.[8] The strong inductive effects of substituents on planar ligands are evident from the glyoxime complexes of iron(II). Iron(II) dimethylglyoxime complexes do not coordinate detectable amounts of carbon monoxide at 1 atm of CO pressure and at room temperature, whereas the bisdiphenylglyoxime complexes have CO binding constants of approximately 40.[9] Interestingly, amine ligands such as saturated noncyclic tetradentate amine ligands, which bear little resemblance to porphyrins, form strong Fe–CO bonds as indicated by a CO stretching frequency of 1940 cm^{-1}.[10]

There has been considerable controversy in the past with respect to the structure of "dioxygen" and carbon monoxide in naturally occurring heme complexes. A recent crystallographic study of the picket-fence porphyrin dioxygen complex has confirmed that dioxygen binds in an angular fashion for electronic rather than steric reasons.[11] Crystallographic studies of two native carbon monoxyhemes, one an x-ray study of an insect hemoglobin (erythrocruorin),[12] and the other a neutron diffraction study of myoglobin,[13] have purported to reveal an angular Fe–CO bond of approximately 135–145°. In both instances, steric interactions of the CO with the surrounding protein appear responsible for the nonlinear binding. However, certain aspects of CO binding in natural heme proteins appear to be inconsistent with angular binding. In particular, the higher binding constant in a sterically hindered environment and the decrease in CO stretching frequency (1951 cm^{-1} for hemoglobin vs. 1970 cm^{-1} for isolated iron(II) heme complexes)[14] would not be expected for a angular Fe–CO bond.

We have initiated a program to evaluate the various factors influencing the stability of iron(II) CO complexes and have been examining a number of different ligands in this respect. The iron(II) complexes of the macrocyclic ligand, 6,8,15,17-tetramethyldibenzo[*b,i*][1,4,8,11]tetraazacyclotetradeca-2,4,7,9,12,14-hexaeneato, $C_{22}H_{22}N_4^{2-}$ (I), in

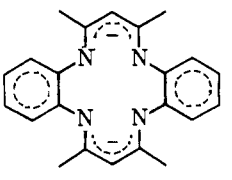

I

particular bind CO very strongly. As part of our overall characterization of these complexes, we have determined the crystal and molecular structure of three iron(II) carbonyl complexes to compare the coordination geometry of the iron with that observed in porphyrin complexes. The complexes chosen for this study have the 14-membered dianionic macrocyclic ligand, I, in common and differ only in the nature of the axial base. One complex is especially noteworthy because it has no axial base, i.e., it is a stable five-coordinate Fe(II)–CO complex. The other two carbonyl complexes have weakly bound molecules of either pyridine or hydrazine in the sixth position. The CO is bound very strongly in these complexes as

indicated by high stability constants (even at CO concentrations as low as 20 ppm, the Fe(II) species appear to be nearly 100% in the carbonyl form[15]) and low carbonyl stretching frequencies, 1915–1940 cm^{-1}. These three complexes provide an unusual opportunity for observing changes in the coordination parameters associated with CO binding in threevery similar environments for which the characteristics of the axial ligands are expected to be the most influential variables. Full details of the stability constants of these and related Fe(II)–CO complexes will be discussed in a separate paper.

The structural features of particular interest are the following: (1) Fe–CO bond lengths and angles, (2) Fe–N_4 (planar) distances, (3) distance of Fe(II) from the N_4 plane, (4) the trans effect of the CO, and (5) characteristics of the planar ligand (extent of double bond delocalization, conformation, etc.).

Experimental Section

Syntheses. **$[Fe(C_{22}H_{22}N_4)(CO)]\cdot\frac{1}{2}C_7H_8$.** A 20-ml anhydrous CH_3CN solution containing 200 mg of $Fe(C_6H_8N_2)_3(NCS)_2$, $C_6H_8N_2$ = *o*-phenylenediamine, was added to a degassed warm solution of the free ligand, $C_{22}H_{24}N_4$ (100 mg), and 1 ml of triethylamine.[16] The solution turned dark red and precipitation of the four-coordinate iron(II) complex, $[Fe(C_{22}H_{22}N_4)]$, began immediately. The product was filtered under N_2, washed with acetonitrile, and dried in vacuo. The product was then dissolved in hot degassed toluene and carbon monoxide was bubbled through the solution. The solution was stoppered under an CO atmosphere and placed in a refrigerator for 12 h to facilitate precipitation of the carbon monoxide complex. The solution was filtered under nitrogen, washed with acetonitrile, and dried in vacuo.

Anal. Calcd for $[Fe(C_{22}H_{22}N_4)(CO)]\cdot\frac{1}{2}C_7H_8$: C, 67.39; N, 11.87; H, 5.51. Found: C, 67.00; N, 11.50; H, 5.71.

$[Fe(C_{22}H_{22}N_4)(C_5H_5N)(CO)]$. A degassed solution containing 200 mg of $Fe(C_5H_5N)_4Cl_2$ in 15 ml of CH_3CN was added to an CH_3CN solution containing 100 mg of $C_{22}H_{24}N_4$ and 1 ml of pyridine. Carbon monoxide gas was then immediately bubbled through the solution for 5 min. The solution was chilled for several hours in a refrigerator to facilitate crystallization of the product. The solution was then filtered and the product washed with acetonitrile, and then dried in vacuo.

Anal. Calcd for $FeC_{28}H_{27}N_5O$: C, 66.5; N, 13.87; H, 5.35. Found: C, 66.65; N, 13.52; H, 5.30.

$[Fe(C_{22}H_{22}N_4)(NH_2NH_2)(CO)]$. A deoxygenated solution containing 200 mg of Fe(*o*-phenylenediamine)$_3$$(NCS)_2$ in 15 ml CH_3CN was added to a deoxygenated solution containing 100 mg of $C_{22}H_{24}N_4$, 1 ml of triethylamine, and 1 ml of hydrazine in 7 ml of CH_3CN. An intense red color developed immediately upon mixing the two solutions. Carbon monoxide was bubbled through the solution for 5 min. Deoxygenated diethyl ether was added dropwise, via a syringe through a serum cap, until the solution became slightly turbid. The solution was then placed in a refrigerator for several hours to facilitate crystallization. The product was filtered, washed with CH_3CN, and dried in vacuo.

Anal. Calcd or $FeC_{23}H_{26}N_6O$: C, 60.28; N, 18.35; H, 5.68. Found: C, 60.50; N, 18.27; H, 5.23.

Preliminary Crystal Examination. Solutions of the iron(II) carbonyl complexes are extremely sensitive to molecular oxygen and were handled under an inert atmosphere. Crystals of all three complexes were also moderately sensitive to molecular oxygen with detectable decomposition of unprotected solid material occurring within 1 day. To prevent decomposition, all samples were always stored under a nitrogen atmosphere. Crystals were mounted on glass fibers in the usual manner, but immediately covered with several thin coats of epoxy resin. In all cases, data collection was initiated within 24 h of mounting the crystal. The extent of crystal decomposition during data collection was within tolerable limits, less than 12%, and the application of a protective epoxy coating appeared preferable to mounting of the crystal in a capillary.

The physical appearance, as well as precession photographs and Weissenberg photographs, of $[Fe(C_{22}H_{22}N_4)(C_5H_5N)(CO)]$ and $[Fe(C_{22}H_{22}N_4)(CO)]$ indicated high quality crystals well suited for intensity measurements. All crystals of $[Fe(C_{22}H_{22}N_4)(N_2H_4)(CO)]$ were of considerably poorer quality; the sides of the crystals were striated indicating lamenar crystal growth. X-ray photographs and diffractometer scans of individual lattice planes selected from different regions of reciprocal space revealed non-Gaussian peaks with shoulders and widely varying mosaic spreads. However, the best crystal examined was not so poor in crystal quality as to preclude obtaining a satisfactory data set.

Preliminary space group and lattice constants for all crystals were determined from zero and upper layer precession and Weissenberg photographs. The systematic absences observed from photographs of $[Fe(C_{22}H_{22}N_4)(NH_2NH_2)(CO)]$ and the pyridine analogue, $[Fe(C_{22}H_{22}N_4)(py)(CO)]$ uniquely established their space groups as $P2_1/c$ and $Pbca$ (C_{2h}^5, No. 14, and D_{2h}^{15}, No. 61),[17] respectively. Precession photographs of crystals of the five-coordinate complex, $[Fe(C_{22}H_{22}N_4)(CO)]\cdot\frac{1}{2}C_7H_8$, revealed no systematic absences and established a triclinic cell; satisfactory refinement assuming a centric model confirmed $P\bar{1}$ as the correct space group.

Collection and Reduction of X-Ray Intensity Data. Pertinent details of the crystal data, intensity data collection, and degree of refinement are listed in Table I. Only the nonroutine aspects will be elaborated upon. The long *a* axis, 30.91 (1) Å, of the pyridine-containing complex necessitated using narrow scan limits (1.1°) to prevent overlap of the intensity measurements. Despite the high crystal quality and uniform mosaicity of the reflections, the narrow scan limits still resulted in the scans being "cut short", producing artificially high background. The result was a uniform reduction of the net intensities by 2–3% from their true value. Although this method of data collection cannot normally be recommended, it appeared superior to the alternatives of using wider scan limits with the attendant problem of individual scans accumulating intensity from adjacent reflections or of collecting data using Cu Kα radiation and contending with the crystal decomposition that frequently occurs with complexes of this type having large absorption coefficients.[18]

The intensities of all reflections were scaled appropriately in blocks of 100 to compensate for the decline (less than 12%) of intensities observed during the data collection.

The raw data were reduced to intensities (I) and estimated errors (σ_I) using $I = S - tb$ and $\sigma_I = [S + t^2B + k^2(S + tb)^2]^{1/2}$ with S = peak scan counts, B = total background costs, t = ratio of peak to background observation times, and k = instability constant = 0.01.[19] These I's and σ_I's were converted to relative structure factors (F) and estimated errors (σ_F) by $F = \sqrt{I/\mathrm{Lp}}$ and $\sigma_F = [(I + \sigma_I)/\mathrm{Lp}]^{1/2} - (I/\mathrm{Lp})^{1/2}$ with Lp = Lorentz and polarization factors.

Solution and Refinement of the Structures. All structures were solved using the Patterson technique and refined using full-matrix least-squares methods.[20] In the final cycles, a model assuming anisotropic thermal motions for the nonhydrogen atoms was used for the $[Fe(C_{22}H_{22}N_4)(C_5H_5N)(CO)]$ and $[Fe(C_{22}H_{22}N_4)(CO)]$ complexes. Only those atoms showing appreciable anisotropic thermal motion (Fe, N atoms of hydrazine, and the O atom of CO) were refined employing anisotropic thermal parameters for the hydrazine-containing complex. All hydrogen atoms were located on difference Fourier maps obtained near the final stages of refinement for all three structures. The hydrogen atom positions were then calculated assuming idealized geometry with C–H distances of 0.95 and 1.00 Å for aromatic and aliphatic C–H hydrogen atoms, respectively.[21] These atoms were included as fixed contributions in the last cycles of least-squares refinement.

The refinement of each structure was straightforward with the exception of the five-coordinate complex. For this compound, the toluene solvent molecule was observed as an extremely diffuse area of electron density in the vicinity of the inversion center, (0,0.5,0.5). Close inspection of difference Fourier maps indicated fourfold disorder of the toluene molecule. Refinement assuming a model in which the positional and anisotropic thermal parameters of all nonhydrogen atoms were varied and treating the toluene solvent molecule as a rigid body, using 3488 data having F's $\geq 3\sigma(F)$, yielded discrepancy indexes of $R_1 = 6.4$ and $R_2 = 8.0$ at convergence. A difference Fourier map at this stage revealed numerous peaks in the areas between the C–C bonds of the toluene molecule. Since an accurate detailed geometry of the toluene molecule was not of major concern, it appeared that the electron density could be better accounted for by refining the coordinates and anisotropic thermal parameters of the individual atoms of the toluene molecule. The multiplicities of the individual atoms were varied because the methyl groups and the ring carbon atoms were not resolvable due to the nature of the overlap (see Figure 3, of the discussion). Refinement to convergence with this model yielded $R_1 = 4.9$, $R_2 = 5.3$. The final difference Fourier map had a

Table I. Crystal Data and Data Collection Details

	$[Fe(C_{22}H_{22}N_4)CO]\cdot \frac{1}{2}C_7H_8$	$[Fe(C_{22}H_{22}N_4)(C_5H_5N)CO]$	$[Fe(C_{22}H_{22}N_4)(NH_2NH_2)CO]$
Mol wt	472.38	505.41	458.36
a	8.6254 (19)	30.907 (13)	9.422 (2)
b	13.0137 (31)	9.619 (5)	11.015 (1)
c	10.9199 (32)	16.615 (7)	21.264 (4)
α	102.32 (2)	90.0	90.0
β	104.39 (2)	90.0	106.58 (1)
γ	78.60 (2)	90.0	90.0
No. of reflections used to determine cell constants	30	20	17
2θ limits, deg	$40 \leq 2\theta \leq 44$	$32 < 2\theta < 44$	$20 \leq 2\theta \leq 38$
Space group	$P\bar{1}$	$Pbca$	$P2_1/c$
Z	2	8	4
ρ_{calcd}, g/cm^3	1.368	1.359	1.439
Absorption coefficient, cm^{-1}	7.04	6.60	7.63
Dimensions, mm	0.073 × 0.23 × 0.32	0.27 × 0.34 × 0.40	0.075 × 0.20 × 0.30
Diffractometer	Picker FACS-1	Picker FACS-1	Picker FACS-1
λ(Mo, Kα), Å	0.71069	0.71069	0.71069
Monochromator	Graphite crystal	Graphite crystal	Graphite crystal
Takeoff angle, deg	3.0	3.0	3
Method	θ-2θ	θ-2θ	θ-2θ
Scan speed, deg/min	2	2	1
Scan width[a] deg	1.4	1.1	2.0
Background time, s	(20 × 2)	(20 × 2)	(20 × 2)
Standards	3	3	3
Av maximum Deviation of standards	12%[b]	3% (random)	4% (random)
2θ limit	$\theta \leq 55°$	$\theta < 55°$	$\theta \leq 55°$
No. of data collected	4266 (non-standard)	4394 (unique) 4990 (non-standard)	4671 (non-standard)
No. of data used in refinement	3488 [$F \geq 3\sigma(F)$]	3696 [$F \geq 3\sigma(F)$]	2802 [$F \geq 2\sigma(F)$]
Data:parameter ratio	11:1	12:1	20:1
Final R_1[c]	4.9	4.2	7.19
Final R_2[d]	5.3	3.6	5.59

[a] Scan width given is for 2θ at 0°, the scan width was as a function of 2θ to accommodate α_1-α_2 splitting at higher angles. [b] Intensity of the standard reflections gradually decreased by an average of 12% of their original intensity during the data collection. A correction factor based on the decreasing intensities of standard reflections was applied to the intensity data, to scale all data to a common level. [c] $R_1 = \Sigma||F_o| - |F_c||/\Sigma|F_o|$. [d] $R_2 = [\Sigma w(|F_o| - |F_c|)^2/\Sigma w|F_o|^2]^{1/2}$.

noise level of 0.15 e/Å^3 with the highest peaks of density, 0.4 e/Å^3, located in the region of the toluene. The estimated standard deviations for the bond distances of the iron complex are good. The chemically equivalent bond distances agreeing very well indicating a satisfactory level of refinement. The final atomic coordinates and thermal parameters for the three structures are listed in Tables II through IV. See paragraph at the end of this paper regarding supplementary material.

Results and Discussion

General Comments. The Fe(II) complexes of the dianionic tetraaza-macrocyclic ligand I readily form monocarbonyl complexes either in the presence or in the absence of other axial ligands. The strong binding of carbon monoxide in these complexes is indicated by low CO stretching frequencies, 1940, 1935, and 1921 cm^{-1} for the hydrazine, pyridine, and five-coordinate complexes, respectively. The complete absence of an axial ligand changes the CO frequency slightly, lowering it 15 cm^{-1} and demonstrates that a σ-donor ligand trans to the CO is not necessary for the formation of stable Fe(II)-CO complexes of porphyrin-type ligands. These CO stretching frequencies are considerably lower than those of Fe(II)-carbonyl complexes of isolated hemes and porphyrins which are in the range of 1970-1980 cm^{-1} and indicate stronger CO binding for the Fe(II) complexes of I. The π-electron system of I is not as extensive as porphyrins and the negative charges of the ligand are localized to the six-membered chelate rings. Both factors contribute to better π-donor properties for Fe(II) complexes of I.

All Fe(II)-carbonyl complexes of I are very sensitive to molecular oxygen, oxidizing immediately to Fe(III) with the loss of CO. This is in marked contrast to Fe(II) and Ru(II) carbonyl complexes of porphyrins, which have much less tendency to react with O_2. Iron(II)-carbonyl complexes of uncharged macrocyclic ligands containing α-diimine functions are unreactive toward dioxygen, bind CO much more weakly, and have considerably higher CO stretching frequencies, 2000-2040 cm^{-1}.[22,23]

Each structure consists of an Fe(II) complex of I linearly bound to a molecule of carbon monoxide. Two complexes have a weakly bound ligand, hydrazine or pyridine, trans to the CO; the third structure is five coordinate. The inner coordination sphere for each structure is shown in Figure 1; projections down the Fe-CO bond axes illustrating the macrocyclic ligands, together with the important interatomic distances, are shown in Figure 2. Figure 3 presents a side view of each molecule illustrating the nonplanarity of the macrocyclic ligand. The important bond angles for the structures are listed in Table V.

The macrocyclic ligand has gross distortions from planarity, vide infra, with a double saddle-like contour. The nonequivalence of the two sides of the ligand leads to the possibility of geometrical isomerism for five-coordinate complexes and for six-coordinate complexes having nonidentical axial ligands.

The carbon monoxide in two structures, $[Fe(C_{22}H_{22}N_4)(CO)]$ and $[Fe(C_{22}H_{22}N_4)(NH_2NH_2)(CO)]$, is located on the side of the macrocyclic ligand to which the benzenoid rings are tipped. This arrangement is expected because the structural constraints of the ligand (vide infra) lead to a preferred displacement of the metal to this side of the N_4 plane, even in the four-coordinate complex, $[Fe(C_{22}H_{22}N_4)]$.[24] Four other five-coordinate complexes of this ligand have the fifth ligand

Table II. Final Positional and Thermal Parameters[a] of Nonhydrogen Atoms of $[FeL(CO)]\cdot\frac{1}{2}C_7H_8$

Atom	X	Y	Z	β_{11}	β_{22}	β_{33}	β_{12}	β_{13}	β_{23}
FE	0.00017 (5)	−0.18213 (3)	0.12236 (4)	91.3 (7)	45.4 (3)	56.9 (5)	−12.4 (3)	3.4 (4)	8.5 (3)
O	−0.1382 (3)	−0.2451 (2)	0.3009 (3)	207 (6)	133 (3)	115 (3)	−65 (3)	34 (6)	44 (3)
N1	0.2238 (3)	−0.2211 (2)	0.2000 (2)	100 (4)	48 (2)	69 (3)	−12 (2)	−0 (3)	17 (2)
N2	−0.0051 (3)	−0.3063 (2)	−0.0111 (2)	116 (4)	43 (2)	58 (3)	−7 (2)	7 (3)	12 (2)
N3	−0.1920 (3)	−0.1284 (2)	0.0067 (2)	93 (4)	43 (2)	56 (3)	−9 (2)	6 (3)	7 (2)
N4	0.0354 (3)	−0.0448 (2)	0.2253 (2)	88 (4)	50 (2)	58 (3)	−16 (2)	8 (3)	5 (2)
C1	0.3293 (4)	−0.2942 (3)	0.1442 (3)	102 (5)	48 (2)	100 (4)	−0 (3)	11 (4)	30 (2)
C2	0.2792 (4)	−0.3637 (3)	0.0317 (3)	126 (6)	49 (2)	100 (4)	12 (3)	31 (4)	17 (3)
C3	0.1237 (4)	−0.3728 (2)	−0.0411 (3)	159 (6)	42 (2)	69 (3)	0 (3)	20 (4)	12 (2)
C4	−0.1674 (4)	−0.3127 (2)	−0.0789 (3)	131 (5)	50 (2)	51 (3)	−23 (3)	8 (3)	9 (2)
C5	−0.2332 (4)	−0.4049 (3)	−0.1375 (3)	179 (7)	51 (2)	84 (4)	−31 (3)	5 (4)	5 (2)
C6	−0.3964 (5)	−0.3988 (3)	−0.1931 (4)	207 (8)	67 (3)	95 (4)	−68 (4)	−3 (5)	1 (3)
C7	−0.4969 (4)	−0.3024 (3)	−0.1886 (3)	131 (6)	85 (3)	92 (4)	−51 (4)	−10 (4)	13 (3)
C8	−0.4347 (4)	−0.2102 (3)	−0.1264 (3)	116 (6)	65 (3)	74 (3)	−23 (3)	0 (3)	19 (2)
C9	−0.2702 (4)	−0.2133 (2)	−0.0714 (3)	101 (5)	54 (2)	52 (3)	−18 (3)	3 (3)	12 (2)
C10	−0.2402 (3)	−0.0254 (2)	−0.0029 (3)	81 (5)	51 (2)	62 (3)	−5 (3)	14 (3)	14 (2)
C11	−0.1684 (4)	0.0551 (2)	0.0853 (3)	99 (5)	43 (2)	81 (3)	−3 (3)	21 (3)	8 (2)
C12	−0.0418 (4)	0.0485 (2)	0.1943 (3)	101 (5)	46 (2)	73 (3)	−16 (3)	28 (3)	0 (2)
C13	0.1595 (4)	−0.0585 (3)	0.3367 (3)	107 (5)	61 (2)	64 (3)	−33 (3)	2 (3)	8 (2)
C14	0.1754 (4)	0.0068 (3)	0.4571 (3)	165 (7)	74 (3)	74 (4)	−32 (3)	9 (4)	2 (3)
C15	0.2944 (5)	−0.0243 (4)	0.5592 (4)	238 (9)	108 (4)	58 (4)	−51 (5)	−19 (5)	−1 (3)
C16	0.3940 (5)	−0.1198 (4)	0.5442 (4)	224 (9)	119 (4)	80 (5)	−52 (5)	−59 (5)	34 (4)
C17	0.3790 (4)	−0.1865 (3)	0.4272 (4)	146 (7)	81 (3)	97 (4)	−18 (4)	−29 (4)	28 (3)
C18	0.2633 (4)	−0.1564 (3)	0.3216 (3)	103 (5)	63 (3)	67 (3)	−26 (3)	−3 (3)	16 (2)
C19	0.5108 (4)	−0.2995 (3)	0.1930 (4)	121 (6)	76 (3)	139 (5)	5 (3)	8 (4)	29 (3)
C20	0.1140 (5)	−0.4567 (3)	−0.1603 (4)	189 (7)	72 (3)	102 (4)	16 (4)	30 (5)	−3 (3)
C21	−0.3673 (4)	0.0101 (3)	−0.1148 (3)	110 (5)	57 (2)	81 (3)	−12 (3)	7 (3)	20 (2)
C22	0.0058 (4)	0.1533 (3)	0.2684 (3)	177 (7)	53 (3)	93 (4)	−22 (3)	14 (4)	−1 (3)
C23	−0.0831 (4)	−0.2217 (3)	0.2262 (3)	118 (6)	60 (3)	68 (4)	−26 (3)	−6 (4)	9 (2)
C24 (0.95)[b]	0.0209 (12)	−0.5770 (9)	0.5038 (5)	356 (16)	267 (6)	86 (9)	−85 (10)	0 (11)	4 (6)
C25 (0.75)	0.1641 (15)	−0.6035 (9)	0.4975 (7)	478 (27)	199 (8)	122 (12)	−50 (11)	2 (13)	20 (7)
C26 (0.54)	0.2770 (15)	−0.5508 (10)	0.4908 (8)	410 (31)	161 (13)	105 (18)	−42 (20)	−12 (18)	76 (14)
C27 (0.50)	0.2575 (15)	−0.4652 (10)	0.4833 (10)	304 (35)	143 (14)	138 (19)	76 (20)	−1 (19)	21 (15)
C28 (0.88)	0.1299 (16)	−0.4073 (8)	0.4886 (6)	623 (31)	219 (9)	121 (12)	−71 (12)	3 (13)	12 (8)
C29 (0.27)	0.0733 (70)	0.4998 (40)	0.4952 (35)	670 (150)	120 (52)	140 (32)	−50 (82)	2 (65)	15 (25)

[a] The form of anisotropic thermal parameters is $\exp[-h^2\beta_{11} + k^2\beta_{22} + l^2\beta_{33} + 2hk\beta_{12} + 2hl\beta_{13} + 2kl\beta_{23}) \times 10^{-4}]$. [b] Multiplicity.

on the same side as the carbonyl in these two complexes.[25,26] The carbon monoxide of the pyridine complex is found on the opposite side of the macrocyclic ligand, an arrangement that was unexpected and, at first glance, appears to be the least stable thermodynamically. The isolation of this isomer may be a consequence of either of the following. Isomerization during the time required for crystal growth might lead to the precipitation of the least soluble isomer, if the thermodynamic stability of the two forms were not vastly different. (Note: Two routes are available for the isomerization of these complexes. The first is by the CO and pyridine switching sides of the molecule through a dissociative process. The second process involves inversion of the macrocyclic ligand conformation by a "flip-flop" process, in which the methyl groups and benzenoid rings pass by one another. The latter process is the most likely because dissociation of CO from these Fe(II) carbonyl complexes has been shown to occur at a very slow rate.) Alternatively, the observed isomer may actually be the more stable thermodynamically. The strength of the Fe–CO bond is not likely to be a strong function of the particular side of the molecular plane on which the CO is located, but the strength of the iron–pyridine bonding will be because of steric interactions of the α-pyridine hydrogen atoms with the atoms of the macrocyclic ligand. If the same Fe–N(pyridine) distance, 2.088 Å, were to be maintained in the nonobserved isomer, the steric interactions would be substantially larger for several reasons: (a) the Fe atom would be displaced (~0.1–0.2 Å) toward the carbonyl side of the N_4 plane, thus pulling the pyridine closer to the molecular plane, (b) the 2,4-pentanediiminato chelate rings would be tipped toward the pyridine side of the N_4 plane, and (c) even though the four-membered *o*-phenylenediamine chelate rings would be bent in the proper direction for minimal contact with the α-pyridine hydrogen atoms, the extent of this bending is less than for the 2,4-pentanediiminato rings (Table VIII) and would result in shorter contact distances between the pyridine and the macrocyclic ligand than in the observed structure. It should be noted that the isomer obtained is independent of the manner of preparation; i.e., the addition of pyridine to the five-coordinate species leads to the same complex (based upon IR spectra and x-ray powder patterns) that is obtained when first pyridine and then carbon monoxide is added to the four-coordinate complex.

Table VI presents a summary of selected bond parameters for the three carbonyl complexes and a fourth related carbonyl complex previously reported. To facilitate the discussion of the structural details of these complexes, various aspects of the inner coordination sphere and the macrocyclic ligand will be considered separately. Because the coordination geometry about the metal is intimately related to the structure of the macrocyclic ligand, details of the ligands will be considered first.

The Macrocyclic Ligand. Distortions from Planarity. The general structural features for the macrocyclic ligand are very similar for all three complexes. In each, the ligand has a pronounced saddle shape due to the steric interactions of the methyl groups of the 2,4-pentanediiminato chelate ring with the benzenoid rings. The resulting strain is minimized by distribution throughout the macrocyclic ligand framework, although not in a uniform manner. The deviations of the dihedral angles from their ideal value, 0° (or 180°) in a planar structure,

Table III. Final Positional and Thermal Parameters[a] and Their Estimated Standard Deviations in Parentheses of Nonhydrogen Atoms of [FeL(CO)(C_5H_5N)]

Atom	X	Y	Z	β_{11}	β_{22}	β_{33}	β_{12}	β_{13}	β_{23}
FE	0.36132 (1)	0.16129 (4)	0.03041 (2)	6.81 (4)	77.4 (4)	24.9 (1)	−1.1 (1)	1.39 (7)	0.6 (2)
O	0.34252 (8)	0.3389 (2)	0.1651 (1)	23.5 (4)	172 (4)	41 (1)	18.2 (10)	2.7 (5)	−30 (2)
N1	0.30162 (6)	0.1744 (2)	−0.0055 (1)	6.8 (2)	77 (3)	24 (1)	−0.2 (7)	2.3 (4)	1 (1)
N2	0.35367 (6)	−0.0080 (2)	0.0920 (1)	7.6 (2)	81 (3)	24 (1)	0.2 (7)	1.6 (4)	3 (1)
N3	0.42151 (6)	0.1388 (2)	0.0619 (1)	7.4 (2)	102 (3)	27 (1)	−1.2 (7)	0.4 (4)	1 (1)
N4	0.36980 (6)	0.3259 (2)	−0.0349 (1)	7.7 (2)	77 (3)	28 (1)	−3.2 (8)	1.9 (4)	0 (1)
N5	0.37501 (6)	0.0431 (2)	−0.0719 (1)	6.8 (3)	80 (3)	24 (1)	0.4 (7)	1.0 (4)	1 (1)
C1	0.26966 (8)	0.1126 (3)	0.0347 (2)	7.3 (3)	76 (3)	29 (1)	−0.7 (8)	2.7 (5)	−6 (2)
C2	0.27745 (8)	0.0205 (3)	0.0981 (2)	7.5 (3)	97 (4)	31 (1)	−1.6 (9)	4.5 (5)	4 (2)
C3	0.31601 (9)	−0.0396 (3)	0.1251 (2)	10.4 (3)	73 (3)	24 (1)	−1.9 (9)	3.3 (5)	2 (2)
C4	0.39314 (8)	−0.0762 (3)	0.1069 (2)	9.1 (3)	88 (4)	25 (1)	3.6 (9)	0.7 (5)	−2 (2)
C5	0.39804 (9)	−0.2139 (3)	0.1296 (2)	10.2 (4)	100 (4)	45 (2)	1.9 (10)	0.9 (6)	3 (2)
C6	0.43855 (11)	−0.2722 (4)	0.1382 (2)	13.7 (5)	97 (5)	58 (2)	11.0 (13)	−1.2 (7)	12 (2)
C7	0.47455 (11)	−0.1948 (4)	0.1211 (2)	9.3 (5)	146 (5)	65 (2)	15.4 (13)	−1.3 (7)	10 (2)
C8	0.47067 (9)	−0.0588 (3)	0.0954 (2)	8.7 (3)	132 (5)	44 (2)	2.7 (10)	−0.2 (6)	5 (2)
C9	0.43033 (8)	0.0040 (3)	0.0898 (2)	8.2 (3)	98 (4)	26 (1)	2.3 (9)	−0.7 (5)	0 (2)
C10	0.44824 (8)	0.2478 (3)	0.0635 (2)	7.3 (3)	125 (4)	37 (1)	−5.4 (10)	−1.2 (5)	−4 (2)
C11	0.43794 (9)	0.3741 (3)	0.0266 (2)	9.5 (3)	106 (4)	46 (1)	121 (10)	−2.5 (6)	−1 (2)
C12	0.40275 (9)	0.4117 (3)	−0.0218 (2)	10.0 (3)	86 (3)	37 (1)	−5.9 (9)	2.7 (6)	0 (2)
C13	0.33452 (8)	0.3492 (3)	−0.0871 (2)	8.3 (3)	70 (4)	25 (1)	1.4 (9)	1.7 (5)	−2 (2)
C14	0.33446 (9)	0.4354 (3)	−0.1546 (2)	10.4 (4)	86 (4)	33 (1)	−4.9 (10)	2.2 (6)	6 (2)
C15	0.29828 (9)	0.4486 (3)	−0.2023 (2)	13.3 (4)	87 (4)	28 (1)	3.1 (10)	0.7 (6)	12 (2)
C16	0.26223 (9)	0.3706 (3)	−0.1859 (2)	10.5 (4)	113 (4)	32 (1)	6.9 (10)	−1.1 (6)	3 (2)
C17	0.26198 (8)	0.2788 (3)	−0.1220 (2)	7.8 (3)	103 (4)	31 (1)	1.3 (9)	1.1 (5)	5 (2)
C18	0.29738 (8)	0.2671 (3)	−0.0707 (1)	7.8 (3)	66 (4)	25 (1)	1.8 (8)	2.1 (5)	−2 (2)
C19	0.22238 (8)	0.1392 (3)	0.0184 (2)	7.6 (3)	126 (4)	40 (1)	−1.6 (9)	3.2 (5)	6 (2)
C20	0.31137 (9)	−0.1372 (3)	0.1957 (2)	12.2 (4)	118 (4)	36 (1)	1.9 (11)	5.7 (6)	16 (2)
C21	0.49043 (10)	0.2453 (4)	0.1095 (2)	11.2 (4)	152 (5)	69 (2)	−9.0 (13)	−8.0 (7)	0 (3)
C22	0.40415 (10)	0.5585 (3)	−0.0540 (2)	14.7 (4)	111 (4)	57 (2)	−15.8 (12)	−4.5 (7)	12 (2)
C23	0.34991 (9)	0.2663 (3)	0.1122 (2)	9.6 (3)	104 (4)	29 (1)	3.7 (10)	0.6 (5)	3 (2)
C24	0.40867 (8)	0.0748 (3)	−0.1187 (2)	7.5 (4)	108 (4)	30 (2)	−3.0 (12)	1.6 (7)	−0 (2)
C25	0.41938 (8)	0.0018 (3)	−0.1868 (2)	8.5 (3)	156 (4)	26 (1)	1.5 (9)	3.3 (5)	−1 (2)
C26	0.39470 (10)	−0.1098 (3)	−0.2083 (2)	11.8 (4)	134 (5)	27 (1)	8.1 (11)	−0.3 (6)	−13 (2)
C27	0.35974 (9)	−0.1438 (3)	−0.1613 (2)	11.4 (4)	93 (4)	37 (1)	−0.6 (11)	−1.3 (6)	−9 (2)
C28	0.35102 (8)	−0.0654 (3)	−0.0938 (2)	8.8 (3)	86 (4)	32 (1)	−3.4 (9)	1.7 (5)	2 (2)

[a] The form of anisotropic thermal parameters is $\exp[-(h^2\beta_{11} + k^2\beta_{22} + l^2\beta_{33} + 2hk\beta_{12} + 2hl\beta_{13} + 2kl\beta_{23}) \times 10^{-4}]$.

result from differing amounts of single- and double-bond character of various bonds in the macrocyclic ligand. Departures from planarity result principally from twists about the nominally single C–N bonds of the five-membered chelate rings derived from *o*-phenylenediamine and the C–N bonds of the 2,4-pentanediiminato linkages. Selected dihedral angles from the three macrocyclic ligands are compared in Table VII. The extent of the twisting is approximately three times greater for the former C–N bonds and varies from 22.3 (4) to 34.6°, while the twisting about the 2,4-pentanediiminato CN bonds varies from 1.3 (8) to 13.4° for the three structures. The deviations of the remaining dihedral angles from ideality are nominal and no more than a few degrees.

The disrotatory twists about the C–N bonds of the five-membered rings and of the six-membered rings produce a saddle-shape conformation of the ligands rather than a propeller-like conformation which would result from a conrotatory twist about these bonds. It is obvious that the saddle-shape observed will lead to smaller angular strain than the propeller-like conformation.

The effects of the ligand nonplanarity on the positioning of the iron atom relative to the N_4 plane and the extent of the distortion can be most easily understood by considering the intersection angles of selected four-atom planes with the N_4 donor atom plane. These have been tabulated in Table VIII. As apparent from these data and the side views of the molecules (Figure 3), deviations of the ligand from planarity are most pronounced with the five-coordinate structure, least so with the six-coordinate pyridine complex (Table VIII, Figure 4).

The ligand possesses a modest degree of flexibility with respect to its ability to direct the lone pairs at the center of the N_4 donor plane, or to direct them slightly above or below the plane. For the five-coordinate complex, the 2,4-pentanediiminato rings are tipped down approximately 7.5° more than the *o*-phenylenediamine chelate rings are tipped up. This unequal tipping directs the lone pairs out of the N_4 donor plane and toward the side to which the benzenoid rings are tipped. The average angle subtended by the Fe–N_4–Ct angles, where Ct is the center of the N_4 donor plane of the macrocyclic ligand, is 8.69°. Thus, the mismatch in terms of the direction of the

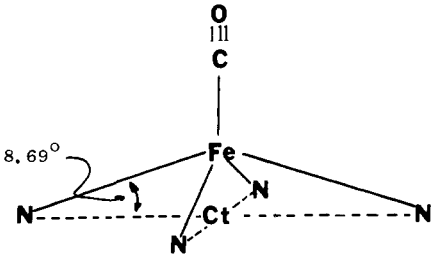

lone pairs and the position of the Fe atom is, at most, no more than a few degrees. For the six-coordinate pyridine complex, the difference in the tip angles of the five- and six-membered chelate rings is much less, 2.5°, and consistent with the donor

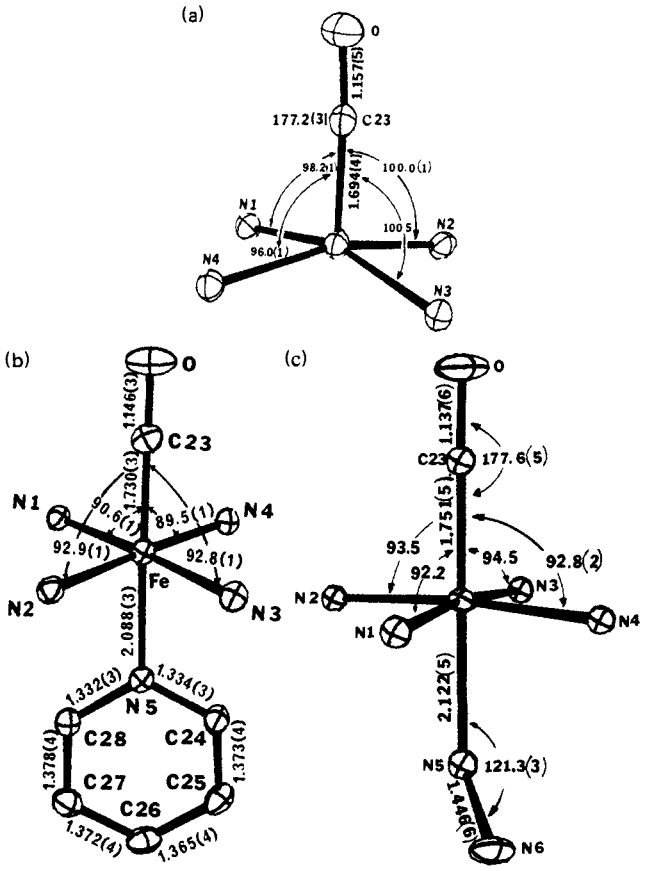

Figure 1. Drawings illustrating the inner coordination sphere of the three carbonyl complexes with selected bond parameters: (a) $[Fe(C_{22}H_{22}N_4)(CO)]$, (b) $[Fe(C_{22}H_{22}N_4)(C_5H_5N)(CO)]$, (c) $[Fe(C_{22}H_{22}N_4)(NH_2NH_2)(CO)]$.

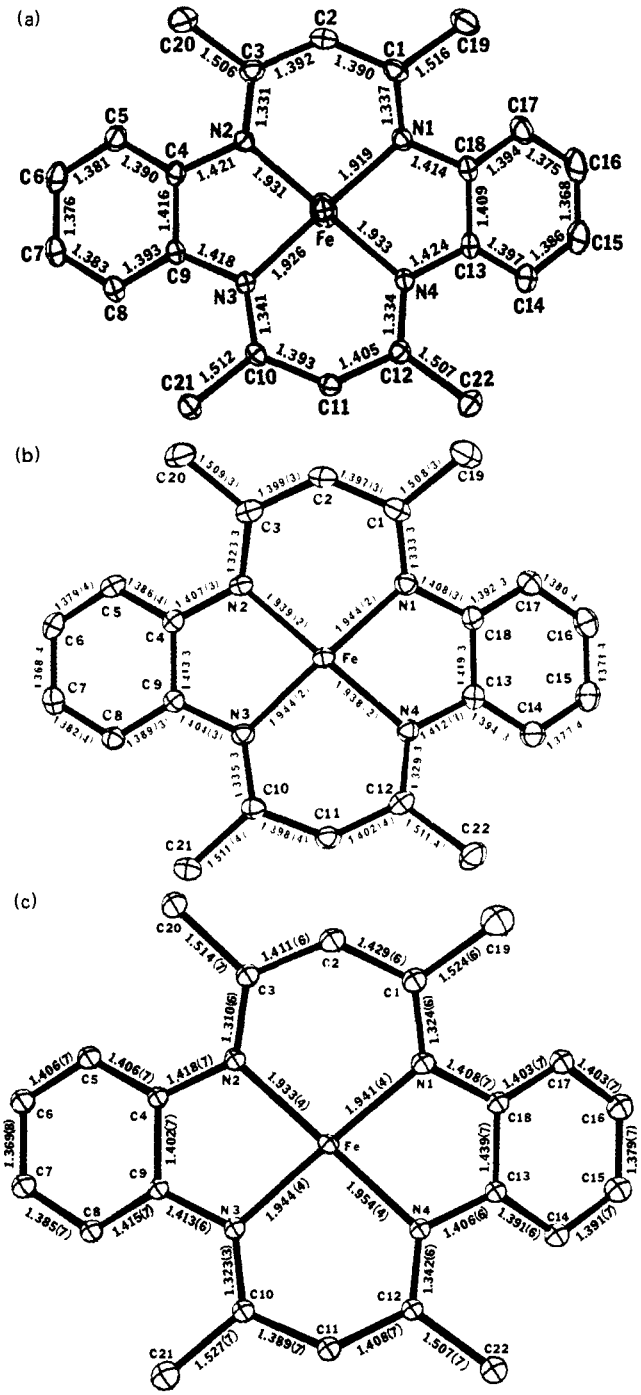

Figure 2. Drawings of the macrocyclic ligand for the three monocarbonyl iron(II) complexes, illustrating the labeling scheme and interatomic distances. The axial ligands and hydrogen atoms have been omitted for clarity of presentation. The thermal ellipsoids have been drawn at the 20% probability level: (a) $[Fe(C_{22}H_{22}N_4)(CO)]$, (b) $[Fe(C_{22}H_{22}N_4)(C_5H_5N)(CO)]$, (c) $[Fe(C_{22}H_{22}N_4)(NH_2NH_2)(CO)]$.

pairs being directed more closely toward the center of the N_4 donor plane and a smaller displacement of the metal from the N_4 plane. Thus the metal moves in concert with the flexing of the ligand such that the N_4 donor electron pairs remain directed at the metal.

Delocalization Patterns. The patterns of delocalization of the macroligand are virtually identical for all three structures. The delocalization is limited primarily to the 2,4-pentanediiminato rings and to the benzenoid rings. It is broken by the C–N bonds of the *o*-phenylenediamine residues, which have predominate single bond character. These C–N bonds have an average length of 1.413 Å for the three structures and may be compared with the expected value of 1.3 Å for a completely delocalized aromatic C–N bond, as observed in a number of pyridine structures.[27] Normal C–N bond lengths for amines bonded to aromatic structures are in the range 1.42–1.46 Å.[28] The C–N single-bond character is attributable to the inherent stability associated with aromatic benzenoid rings and highly delocalized 2,4-pentanediiminato chelate rings and is not a result of the twisting about these bonds that leads to the saddle shape of the ligands. The crystal structure of a Ni(II) complex of a dibenzo[14]annulene ligand devoid of any steric interactions has a C–N bond length, 1.416 Å,[29] comparable to that observed in the structures considered here.

The delocalization about the 2,4-pentanediiminato rings is compatible with that ascribed to aromatic structures. The average C–N bond length and average C–C bond length for the three structures is 1.330 and 1.401 Å, respectively, and within experimental error of accepted aromatic C–N and C–C distances of 1.33 and 1.39 Å, respectively.

The benzenoid rings are clearly aromatic in all three structures, but the bond lengths are significantly different for the four distinct types of C–C bonds in each ring. The longest C–C bonds are those attached to the N atoms and have an average value of 1.416 Å. The C–C bonds become progressively shorter toward the opposite side of the benzenoid rings, with the shortest having an average value of 1.372 Å. These differences are probably both steric and electronic in origin; the two effects are not easily separated in these structures. The observed differences do not represent partial localization of the double bonds, since the bond lengths do not alternate around the ring. Alternation of bond lengths in an Fe(II)

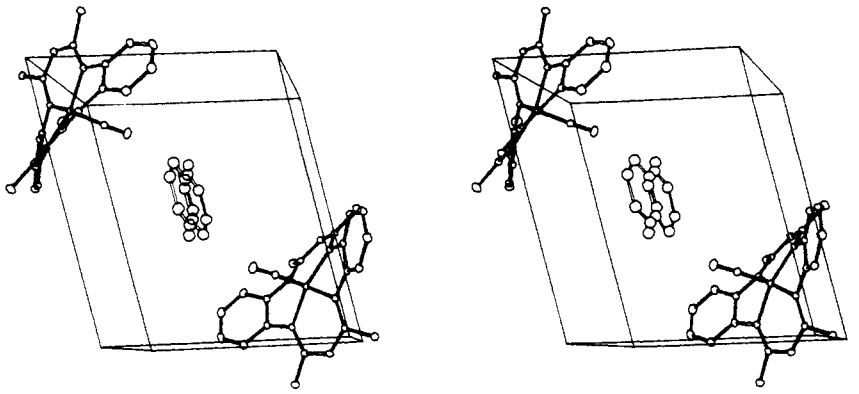

Figure 3. Diagram illustrating the arrangement of the $[Fe(C_{22}H_{22}N_4)(CO)]$ molecules in the unit cell and the nature of the disorder of the toluene solvent molecule.

Table IV. Final Positional and Thermal Parameters of Nonhydrogen Atoms of $[FeL(CO)(N_2H_4)]$

Atoms	*X*	*Y*	*Z*	*B*, Å^2
Fe	0.15932 (8)	0.01941 (7)	0.30771 (4)	*a*
O	0.2978 (6)	−0.2154 (4)	0.3116 (3)	*a*
N1	0.2426 (4)	0.0408 (4)	0.4018 (2)	2.5 (1)
N2	0.3140 (4)	0.1058 (4)	0.2813 (2)	2.1 (1)
N3	0.0619 (4)	0.0148 (4)	0.2141 (2)	2.2 (1)
N4	−0.0045 (4)	−0.0491 (4)	0.3340 (2)	2.1 (1)
N5	0.0567 (5)	0.1917 (4)	0.3047 (2)	2.7 (1)
N6	−0.0083 (6)	0.2292 (4)	0.3555 (3)	*a*
C1	0.3389 (6)	0.1282 (5)	0.4262 (3)	2.7 (1)
C2	0.4126 (6)	0.1926 (5)	0.3889 (3)	2.9 (1)
C3	0.4105 (6)	0.1791 (5)	0.3228 (3)	2.5 (1)
C4	0.3032 (6)	0.0854 (5)	0.2147 (3)	2.1 (1)
C5	0.4125 (6)	0.0999 (5)	0.1831 (3)	2.8 (1)
C6	0.3894 (6)	0.0695 (5)	0.1172 (3)	3.1 (1)
C7	0.2573 (6)	0.0174 (5)	0.0824 (3)	3.1 (1)
C8	0.1458 (6)	−0.0033 (5)	0.1129 (2)	2.6 (1)
C9	0.1641 (5)	0.0337 (5)	0.1779 (2)	2.2 (1)
C10	−0.0837 (6)	0.0063 (5)	0.1896 (2)	2.3 (1)
C11	−0.1792 (5)	−0.0184 (5)	0.2296 (2)	2.4 (1)
C12	−0.1420 (4)	−0.0461 (4)	0.2972 (2)	2.1 (1)
C13	0.0424 (6)	−0.0901 (5)	0.3999 (3)	2.3 (1)
C14	−0.0251 (6)	−0.1839 (5)	0.4258 (3)	3.0 (1)
C15	0.0429 (7)	−0.2239 (5)	0.4902 (3)	3.6 (1)
C16	0.1744 (7)	−0.1750 (6)	0.5262 (3)	3.6 (1)
C17	0.2448 (6)	−0.0848 (5)	0.5010 (3)	3.0 (1)
C18	0.1773 (6)	−0.0402 (5)	0.4370 (3)	2.4 (1)
C19	0.3697 (7)	0.1688 (6)	0.4975 (3)	4.4 (1)
C20	0.5241 (6)	0.2552 (5)	0.3034 (3)	3.1 (1)
C21	−0.1658 (6)	0.0287 (6)	0.1177 (3)	3.5 (1)
C22	−0.2725 (6)	−0.0649 (5)	0.3243 (3)	3.0 (1)
C23	0.2452 (6)	−0.1220 (5)	0.3094 (3)	2.4 (1)

Anisotropic Thermal Parameters[a]

Atoms	β_{11}	β_{22}	β_{33}	β_{12}	β_{13}	β_{23}
Fe	66.5 (9)	33.8 (6)	10.4 (2)	1.8 (8)	4.8 (3)	−1.0 (4)
O	235 (9)	67 (5)	52 (2)	65 (6)	64 (4)	12 (3)
N6	181 (6)	68 (5)	27 (2)	22 (6)	45 (4)	−7 (3)

[a] Anisotropic thermal parameters are of the form $\exp[-(h^2\beta_{11} + k^2\beta_{22} + l^2\beta_{33} + 2hk\beta_{12} + 2hl\beta_{13} + 2kl\beta_{23}) \times 10^{-4}]$.

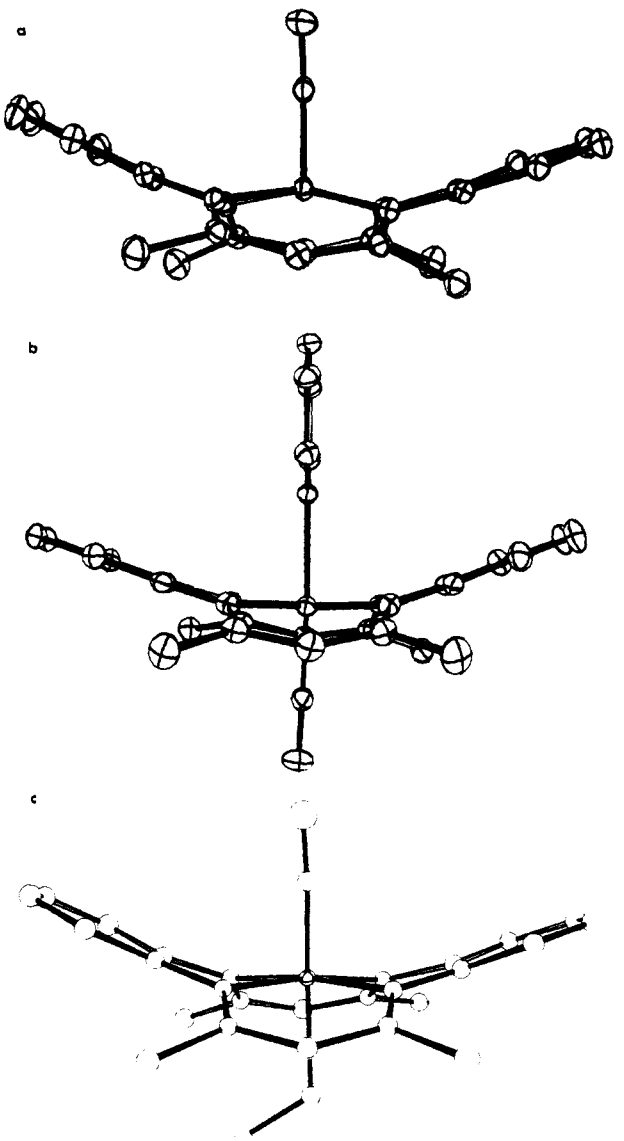

Figure 4. Side view of the three iron(II) carbon monoxide complexes illustrating the double saddle-like shape of the macrocyclic ligands: (a) $[Fe(C_{22}H_{22}N_4)(CO)]$, (b) $[Fe(C_{22}H_{22}N_4)(C_5H_5N)(CO)]$, (c) $[Fe(C_{22}H_{22}N_4)(NH_2NH_2)(CO)]$.

complex containing an oxidized form of *o*-phenylenediamine, *o*-benzoquinonediimine, has been observed.

Inner Coordination Sphere. The Fe(II)-C(CO) bond lengths vary from 1.689 (5) to 1.751 (6) Å and are in the range normally observed for first-row transition-metal carbonyl complexes. The five-coordinate complex has the shortest Fe-C(CO) distance, 1.689 (6) Å, and also the lowest CO stretching frequency, indicating a stronger Fe-CO bond in the absence of a sixth ligand. The Fe-C bond lengths of the two six-coordinate structures, although significantly different on

Table V. Bond Angles (deg)

	[FeL(CO)]	[FeL(CO)-(C_5H_5N)]	[FeL(CO)-(N_2H_4)]		[FeL(CO)]	[FeL(CO)-(C_5H_5N)]	[FeL(CO)-(N_2H_4)]
N1-Fe-N2	94.2 (1)	95.8 (1)	97.1 (2)	C5-C4-C9	119.5 (3)	119.2 (2)	117.9 (5)
N1-Fe-N3	61.3 (1)	176.6 (1)	173.2 (2)	C4-C5-C6	120.1 (3)	121.1 (3)	122.2 (5)
N1-Fe-N4	82.6 (1)	84.4 (1)	82.6 (2)	C5-C6-C7	120.8 (4)	119.7 (3)	119.9 (5)
N2-Fe-N3	82.6 (1)	83.2 (1)	83.7 (2)	C6-C7-C8	119.8 (3)	120.6 (3)	120.0 (5)
N2-Fe-N4	164.0 (1)	177.6 (1)	173.7 (2)	C7-C8-C9	120.7 (3)	120.7 (3)	120.7 (5)
N3-Fe-N4	95.3 (1)	96.5 (1)	95.9 (2)	C4-C9-N3	113.5 (2)	114.4 (2)	114.9 (4)
N5-Fe-N1		88.7 (1)	88.2 (2)	C4-C9-C8	118.9 (3)	118.6 (3)	119.1 (5)
N5-Fe-N2		89.9 (1)	85.8 (2)	N3-C9-C8	127.1 (3)	126.8 (3)	125.7 (5)
N5-Fe-N3		88.0 (1)	85.1 (2)	N3-C10-C11	121.9 (3)	122.2 (2)	122.5 (6)
N5-Fe-N4		87.8 (1)	87.9 (2)	N3-C10-C21	122.2 (3)	122.1 (3)	123.7 (4)
C23-Fe-N1	98.2 (1)	90.6 (1)	92.2 (2)	C11-C10-C21	115.7 (3)	115.6 (3)	113.7 (5)
C23-Fe-N2	100.0 (1)	92.9 (1)	93.5 (2)	C10-C11-C12	129.9 (3)	130.8 (3)	129.1 (5)
C23-Fe-N3	100.5 (1)	92.8 (1)	94.5 (2)	C11-C12-N4	121.8 (3)	121.9 (3)	122.1 (5)
C23-Fe-N4	96.0 (1)	89.5 (1)	92.8 (2)	C11-C12-C22	115.4 (3)	115.0 (3)	115.2 (4)
C23-Fe-N5		177.2 (1)	179.2 (2)	N4-C12-C22	122.7 (3)	123.0 (3)	122.7 (4)
Fe-N1-C1	125.0 (2)	121.3 (2)	121.4 (4)	N4-C13-C14	127.4 (3)	126.2 (2)	124.9 (5)
Fe-N1-C18	109.9 (2)	111.5 (2)	110.1 (3)	N4-C13-C18	112.9 (2)	114.7 (2)	114.1 (5)
C1-N1-C18	124.9 (2)	126.8 (2)	127.3 (5)	C14-C13-C18	119.3 (3)	119.0 (2)	120.5 (5)
Fe-N2-C3	125.5 (2)	121.3 (2)	121.6 (4)	C13-C14-C15	119.7 (3)	121.3 (3)	118.7 (5)
Fe-N2-C4	109.8 (2)	112.3 (2)	111.5 (3)	C14-C15-C16	120.7 (3)	119.6 (3)	120.7 (6)
C3-N2-C4	124.6 (2)	125.7 (2)	126.8 (4)	C15-C16-C17	120.7 (4)	120.5 (3)	121.5 (6)
Fe-N3-C9	110.6 (2)	112.2 (2)	111.1 (3)	C16-C17-C18	120.1 (3)	121.2 (2)	119.2 (5)
Fe-N3-C10	124.5 (2)	120.7 (2)	122.6 (3)	C13-C18-N1	114.2 (2)	115.2 (2)	114.3 (5)
C9-N3-C10	124.8 (2)	126.8 (2)	126.1 (4)	C13-C18-C17	119.5 (3)	118.2 (2)	119.4 (5)
Fe-N4-C12	124.9 (2)	121.3 (2)	123.4 (4)	N1-C18-C17	125.9 (3)	126.5 (2)	125.8 (5)
Fe-N4-C13	109.7 (2)	111.7 (2)	111.1 (3)	Fe-C23-O	177.2 (3)	178.2 (3)	177.6 (5)
C12-N4-C13	125.3 (2)	126.4 (2)	125.2 (4)	Fe-N5-N6			121.3 (3)
N1-C1-C2	121.8 (3)	122.2 (2)	123.1 (5)	Fe-N5-C24		120.5 (2)	
N1-C1-C19	122.0 (3)	123.5 (2)	121.1 (5)	Fe-N5-C28		122.4 (2)	
C2-C1-C19	116.0 (3)	114.2 (2)	115.7 (5)	C24-N5-C28		117.0 (2)	
C1-C2-C3	129.6 (3)	130.6 (2)	130.5 (5)	N5-C24-C25		123.5 (3)	
C2-C3-N2	121.6 (3)	121.4 (2)	122.4 (5)	C24-C25-C26		118.9 (3)	
C2-C3-C20	115.4 (3)	115.2 (2)	113.9 (5)	C25-C26-C27		118.7 (3)	
N2-C3-C20	122.9 (3)	123.3 (2)	123.7 (5)	C26-C27-C28		119.1 (3)	
N2-C4-C5	126.8 (3)	126.0 (3)	128.1 (5)	C27-C28-N5		122.9 (2)	
N2-C4-C9	113.4 (3)	114.5 (3)	113.8 (4)				

Table VI. Summary of Bond Parameters for Four Iron(II) Carbon Monoxide Complexes of Macrocyclic Ligands

	Complex			
Parameter	[FeL(CO)][a]	[FeL(N_2H_4)(CO)]	[FeL(C_5H_5N)(CO)]	[FeL'(CH_3)(CO)][b]
CO bond length	1.157 (2) Å	1.137 (6) Å	1.146 (3) Å	1.167 (6) Å
ν_{CO}	1915 cm^{-1}	1940 cm^{-1}	1930 cm^{-1}	1925 cm^{-1}
FeCO angle	177.2 (3)°	177.6 (5)°	178.2 (3)°	180.0 (0)°
Av Fe-N (planar) distance	1.927 (4) Å	1.944 (4) Å	1.941 (2) Å	1.900 (2) Å
Fe-trans ligand distance		2.122 (5) Å (NH_2NH_2)	2.088 (3) Å (C_5H_5N)	2.077 (5) Å (CH_3^-)
Distance of Fe from N_4 plane	0.29 Å	0.11 Å	−0.05 Å	0.187 Å

[a] L = $C_{22}H_{22}N_4^{2-}$. [b] L' = $C_{10}H_{19}N_8^-$, see ref 30.

the basis of the estimated standard deviations, are not directly comparable. The constraints governing the bond parameters for "top" vs. "bottom" binding of carbon monoxide with respect to the two sides of this ligand are different; the interaction of the axial ligands with the iron and the macrocyclic ligand are highly dependent upon the distance of the metal from the N_4 plane of the macrocyclic ligand and the side of the ligand to which it is displaced.

Very few related Fe(II)-CO structures have been reported that may be compared with the above Fe(II)-CO complexes. The most closely related structure is a bis α-diimine macrocyclic complex containing CO and a CH_3 group in the axial sites.[30] The Fe-C distance was found to be 1.772 (5) Å, slightly longer than observed for the three complexes being considered. However, the Fe-CO bond in the latter complex must also be quite strong in view of the low CO stretching frequency, 1925 cm^{-1}. The Fe-CO angle in all the complexes deviates only marginally from being linear; slight deviations from 180° result from packing interactions.

Ruthenium(II)[31-35] and Os(II)[36] form monocarbonyl complexes with porphyrins analogous to the Fe(II)-CO complexes considered here. Dicarbonyl complexes of Ru(II) porphyrins have also been characterized.[37] Although the original studies of the Ru(II)-CO porphyrins purported them to be five-coordinate, more recent NMR and x-ray structural studies have shown them to be six-coordinate with the sixth ligand very weakly held.[38,39] The CO stretching frequencies for ruthenium porphyrin monocarbonyl complexes, 1920–1960

Table VII. Selected Dihedral Angles (deg)

Planes defined by	[Fe($C_{22}H_{22}N_4$)-(py)(CO)]	[Fe($C_{22}H_{22}N_4$)-(CO)]	[Fe($C_{22}H_{22}N_4$)-(N_2H_4)(CO)]
C19,C1,N1-C1,N1,C18	3.2 (4)	13.4 (5)	12.3 (8)
C1,N1,C18-N1,C18,C17	22.3 (4)	34.6 (6)	32.1 (8)
C20,C3,N2-C3,N2,C4	11.8 (4)	6.7 (6)	1.3 (8)
C3,N2,C4-N2,C4,C5	28.1 (4)	34.5 (6)	23.8 (8)
C21,C10,N3-C10,N3,C9	10.4 (4)	11.3 (5)	6.5 (8)
C10,N3,C9-N3,C9,C8	26.8 (4)	31.1 (5)	29.1 (8)
C22,C12,N4-C12,N4,C13	8.32 (4)	6.5 (5)	11.5 (8)
C12,N4,C13-N4,C13,C14	25.3 (4)	32.2 (6)	33.6 (8)

Table VIII. Intersection Angles of the N_4 Donor Atom Plane with Other Selected Planes

Atoms defining the planes N_1,N_2,N_3,N_4 with:	Intersection angles, deg [Fe-($C_{22}H_{22}N_4$)-(CO)]	[Fe-($C_{22}H_{22}N_4$)-(N_2H_4)(CO)]	[Fe-($C_{22}H_{22}N_4$)-(py)CO]
N1,C1,C3,N3	24.88	20.63	19.81
N3,C10,C12,N4	23.44	22.34	19.70
N2,C4,C9,N3	16.49	15.71	18.34
N1,C18,C13,N4	17.32	18.85	16.17
C4,C5,C6,C7,C8,C9	22.35	19.50	22.33
1c13,C14,C15,C16,C-17,C18	23.84	26.04	19.02

cm^{-1}, are lower than Fe(II) carbonyl porphyrins; that of Os(OEP)CO·py is lower still, 1902 cm^{-1}. Dicarbonyl complexes of Ru(II) porphyrins have higher CO stretching frequencies, 1990–2050 cm^{-1},[37] because of diminished π back-bonding resulting from two carbonyl functions competing for Ru(II) π-orbitals. The Ru-C(CO) distances, 1,838 (9) Å, and 1.77 (2) Å for the [Ru(TPP)(py)(CO)]·1.5C_7H_8[38] and [Ru(TPP)(EtOH)(CO)][39] complexes, respectively, are only slightly longer than observed for our Fe-CO complexes. The Os-C(CO) distance of a novel Os porphodimethene carbonyl is 1.828 Å.[36]

Displacement of the Iron from the N_4 Plane. The displacement of a metal from the N_4 plane of a macrocyclic ligand is a function of the various constraints of the macrocyclic ligand and the number of axial ligands (one or two) and their relative bonding strength. In the complexes under consideration, the Fe atom is displaced significantly from the N_4 donor plane. The displacements of 0.11 and 0.29 Å for the hydrazine complex and the five-coordinate complex, respectively, result from the combined effects of the strong π donor-acceptor character of the Fe-CO bond and from steric interactions within the macrocyclic ligand. The Fe atom of the six-coordinate pyridine complex is displaced only slightly, 0.05 Å, from the N_4 plane, but to the opposite side of the plane. Thus the very strong binding of CO can pull the Fe(II) further out of the N_4 plane, as in the five-coordinate complex (as compared to the four-coordinate Fe(II) complex[24]), or pull the Fe(II) atom through to the other side of the macrocyclic ligand plane when coordinated to the least favorable side of the macrocyclic ligand, as in the pyridine complex.

The displacement of the Fe from the N_4 plane in two of our structures is larger than for the ruthenium carbonyl porphyrin complex, for which a displacement of 0.068 Å from the N_4 plane of the porphyrin was found.[39] The Os(II) ion of [Os(porphodimethene)CO(py)] is displaced 0.18 Å out of the N_4 plane toward the carbonyl ligand.[36]

Bonding Trans to Carbon Monoxide. The Fe-N (axial base) distances, 2.122 (5) and 2.088 (3) Å for the hydrazine and pyridine complexes, respectively, are unusually long. Normal low-spin iron(II)-nitrogen distances are predicted to be about 2.00 Å.[40] The orientation of the pyridine molecule minimizes the steric interactions of the α-hydrogen atoms of the pyridine with the macrocyclic ring carbon and nitrogen atoms. Thus the pyridine hydrogen atoms are pointed directly toward the center of the 2,4-pentanediiminato chelate ring (Figure 4b). The dihedral angle defined by the planes composed of atoms C2-Fe-N5-C11and atoms Fe-N5-C24-C25 are zero to within experimental error. The pyridine hydrogen atoms are about 1.0 Å away from the plane defined by the atoms of the 2,4-pentanediiminato chelate rings. The closest contacts of these hydrogen atoms are with the macrocyclic nitrogen atoms with distances of 2.67, 2.77, 2.78, and 2.81 Å. The closest contacts to carbon atoms range from 2.92 to 3.13 Å. The N···H distances are shorter than the sum of the van der Waals radii for hydrogen (1.20 Å) and aromatic nitrogen (1.70 Å) of 2.90 Å. However, if the Fe-N bond is strong as in [Fe(TPP)(imidazole)$_2$], which has Fe-N(imidazole) distances of 1.957 (4) and 1.991 (5) Å, closer contacts involving the α-hydrogen atoms of 2.56 and 2.58 Å occur.[41] Thus in the case of the pyridine ligand, the relatively long Fe-N(pyridine) distance of 2.088 Å may partially be attributable to steric interactions. Additional evidence for the coordinated CO contributing to weak binding of the remaining axial ligand is provided by the long Fe-N(hydrazine) distance of 2.122 (5) Å, for which there are no major nonbonding interactions, and the fact that the five-coordinate complex is also obtained from acetonitrile solution.

Similar lengthening of Ru(II)-N(pyridine) and Os(II)-N(pyridine) bond lengths have been observed. The Ru-N(py) and Ru-O(EtOH) distances are 2.193 (4) and 2.21 (2) Å, respectively, as compared to the Ru-N(porphyrin) distance of 2.052 (9) Å. The Os-N(pyridine) distance of a porphyrin derivative was found to be 2.230 Å. In all cases, steric interactions of the α-hydrogen atoms of the pyridine with the planar ligand in all cases appear to preclude shorter metal-pyridine distances.

"In-Plane" Iron(II)-Nitrogen Distances. The "in-plane" Fe(II)-N distances vary from 1.927 (4) Å for the five-coordinate complex to 1.944 (4) Å for the six-coordinate hydrazine complex. The shortest distances, both for Fe(II)-N and Fe(II)-C bonds, are expected for the five-coordinate complex, since some overall tightening of all the iron bonds will occur to compensate for the absence of a sixth ligand. Consistent with this viewpoint, the average Fe-N distance of the four-coordinate [Fe($C_{22}H_{22}N_4$)] complex is shorter still, 1.917 (3) Å.[24]

The Fe(II)-N distances are significantly shorter than observed in the structural investigations of the Fe(II) porphyrin complexes, for which the shortest Fe(II)-N(porphyrin) distances are observed for the low-spin complexes and vary from 2.004 (4) Å[42] for the six-coordinate bis-piperidine complex to 1.972 (4) Å for the four-coordinate, $S = 1$, tetraphenylporphyrin complex.[43]

Conclusions

The dibenzotetraaza[14]annulene ligand presents a significantly smaller coordination radius than do porphyrin ligands, and leads to Fe(II)-N distances of about 1.94 Å, 0.06 Å shorter than found for low-spin iron(II) porphyrin complexes. The delocalization of the macrocyclic ligand is limited

to the benzenoid groups and the 2,4-pentanediiminato chelate rings, and is broken by the twist C–N bonds (of the *o*-phenylenediamine residues) resulting from steric interactions within the macrocyclic ligand. The negative charges of the ligand are thus localized to the six-membered chelate rings, stabilizing the Fe(III) state, and account for the extremely oxygen-sensitive nature of our Fe(II)–CO complexes as opposed to the oxygen insensitivity of Fe(II)–CO porphyrin and heme complexes.

In view of the low CO stretching frequencies observed for our Fe–CO complexes and the similarity of the CO stretching frequencies observed with the ruthenium monocarbonyl porphyrin complexes, dicarbonyl formation with the Fe(II) complexes of I might be expected. Our failure to observe any dicarbonyl complex formation (up to several atmospheres of CO pressure) can be attributed, in large part, to the preferential displacement of the Fe atom to one side of the ring and its effect of reducing the affinity for a sixth ligand.

The binding of CO to the Fe(II) also produces a strong trans effect, as indicated by abnormally long Fe–N (trans ligand) distances, even in the hydrazine complex where steric interactions are absent. The characterization of the five-coordinate Fe–CO complex demonstrates that a σ-donor ligand trans to the CO is unnecessary for strong and stable Fe(II)–CO bonding.

The carbonyl complexes of hemoglobin and myoglobin are also likely to have abnormally long Fe–N (trans to CO) distances. This undoubtedly will effect the position of the iron(II) with respect to the heme ring and the globular protein and be a contributing factor in the cooperativity of CO binding in hemoglobin.

Acknowledgment. This research was supported in part by the National Institutes of Health, Grant No. HL14827.

Supplementary Material Available: A list of structure factors amplitudes and coordinates of the hydrogen atoms used in the structural refinements (60 pages). Ordering information is given on any current masthead page.

References and Notes

(1) Address correspondence to this author at the Department of Chemistry, Florida State University Tallahassee, Fla. 32306.
(2) J. P. Collman, R. R. Gagne, T. R. Halbert, J. C. Marchan, and C. R. Reed, *J. Am. Chem. Soc.*, **95**, 7870 (1973); J. P. Collman, R. R. Gagne, and C. R. Reed, *ibid.*, **96**, 2630 (1974); J. P. Collman, R. R. Gagne, C. A. Reed, T. R. Halbert, G. Lang, and R. T. Robinson, *ibid.*, **97**, 1427 (1975); J. P. Collman, J. I. Braurman, T. R. Halbert, and K. S. Suslick, *Proc. Natl. Acad. Sci. U.S.A.*, **73**, 3333 (1976); J. Almog, J. E. Baldwin, R. L. Dyer, and M. Peters, *J. Am. Chem. Soc.*, **97**, 7049 (1975); J. Almog, J. E. Baldwin, and J. Huff, *ibid.*, **97**, 227 (1975); J. E. Baldwin and J. Huff, *ibid.*, **95**, 5757 (1973); J. Almog, J. E. Baldwin, R. L. Dyer, J. Huff, and C. J. Wickerson, *ibid.*, **96**, 5600 (1974).
(3) C. K. Chang and T. G. Traylor, *Proc. Natl. Acad. Sci. U.S.A.*, **70**, 2647 (1973); C. K. Chang and T. G. Traylor, *J. Am. Chem. Soc.*, **95**, 5810, 8479 (1973); W. S. Brinigar, C. K. Chang, J. Geibel, and T. G. Traylor, *ibid.*, **96**, 5598 (1974).
(4) D. L. Anderson, C. J. Weschler, and F. Basolo, *J. Am. Chem. Soc.*, **96**, 5600 (1974); *J. Chem. Soc., Chem. Commun.*, 757 (1974).
(5) M. Keyes, H. Mizukami, and R. Lumry, *Anal. Biochem.*, **18**, 126 (1967).
(6) F. Antonini and M. Brunori, "Hemoglobin and Myoglobin and Their Reaction with Ligands", North Holland Publishing Co., Amsterdam, 1971, pp 225, 261.
(7) W. S. Caughey, J. O. Alben, and C. A. Beaudreau, "Oxidases and Related Systems", T. E. King, H. S. Mason, and M. Morrison, Ed., Wiley, New York, N.Y., 1965, p 97.
(8) D. V. Stynes and B. R. James, *J. Am. Chem. Soc.*, **96**, 2733 (1974).
(9) L. V. Vaska and T. Yamaji, *J. Am. Chem. Soc.*, **93**, 6673 (1971).
(10) L. R. Melby, *Inorg. Chem.*, **9**, 2186 (1970).
(11) J. P. Collman, R. R. Gagne, C. A. Reed, W. T. Robinson, and G. A. Rodley, *Proc. Natl. Acad. Sci. U.S.A.*, **71**, 1326 (1974).
(12) R. Huber, O. Epp, and H. Formanek, *J. Mol. Biol.*, **52**, 349 (1970).
(13) J. C. Norvell, A. C. Nunes, and B. P. Schoenborn, *Science*, **190**, 568 (1975).
(14) J. O. Alben and W. S. Caughey, *Biochemistry*, **7**, 175 (1968); W. S. Caughey, J. O. Alben, S. McCoy, S. M. Boyer, S. Charache, and P. Hatway, *ibid.*, **8**, 59 (1969).
(15) M. Suh and V. L. Goedken, submitted for publication.
(16) All elemental analyses were determined by Galbraith Laboratories, Inc., Knoxville, Tenn.
(17) "International Tables for X-Ray Crystallography", Vol. I., Kynoch Press, Birmingham, England, 1973.
(18) The quantum yield for the photodissociation of carbon monoxide from heme proteins is very high (T. Bücher and E. Negelein, *Biochem. Z.*, **311**, 163 (1942); T. Bücher and J. Kaspers, *Biochim. Biophys. Acta*, **1**, 21 (1947); R. W. Noble, M. Brunori, J. Wyman, and E. Antonini, *Biochemistry*, **6**, 1216 (1967)). Since the Fe(II)–CO complexes of I absorb intensely in the visible and UV spectral range, the probability of appreciable photodissociation and crystal decomposition following prolonged exposure to Cu Kα X-radiation appeared high. The photochemistry of these complexes is currently under investigation.
(19) P. Corfield, R. Doedens, and J. Ibers, *Inorg. Chem.*, **6**, 197 (1967).
(20) Computations were performed on an IBM 370 computer with the aid of the following programs: Zalkin's FORDAP Fourier program, Busing and Levy's ORFFE error function program, and Ibers NUCLS least-squares program. Plots of the structures were drawn with the aid of C. K. Johnson's ORTEP. Neutral atom scattering factors were taken from D. T. Cromer and J. B. Mann, *Acta Crystallogr., Sect. A*, **24**, 321 (1968). Hydrogen atom scattering factors were taken from "International Tables for X-Ray Crystallography", Vol. III, Kynoch Press, Birmingham, England, 1962. Anomalous scattering corrections were applied to heavy atoms and were taken from D. T. Cromer, *Acta Crystallogr.*, **18**, 17 (1965).
(21) M. R. Churchill, *Inorg. Chem.*, **12**, 1213 (1973).
(22) V. L. Goedken, Y.-A. Park, S.-M. Peng, and J. Molin-Norris, *J. Am. Chem. Soc.*, **96**, 7693 (1974).
(23) D. Baldwin, R. Pfeiffer, D. Reichgott, and N. Rose, *J. Am. Chem. Soc.*, **94**, 3397 (1972).
(24) V. L. Goedken, J. J. Pluth, S.-M. Peng, and B. Bursten, *J. Am. Chem. Soc.*, **98**, 8014 (1976).
(25) M. C. Weiss, B. Bursten, S.-M. Peng, and V. L. Goedken, *J. Am. Chem. Soc.*, **98**, 8021 (1976).
(26) V. L. Goedken, S.-M. Peng, and Y.-A. Park, *J. Am. Chem. Soc.*, **96**, 284 (1974).
(27) R. W. G. Wyckoff, "Crystal Structures", Vol. VI, Part 1, Wiley, New York, N.Y., 1969, pp 129, 191; V. L. Goedken and G. C. Christoph, *Inorg. Chem.*, **12**, 2316 (1973).
(28) G. C. Christoph and V. L. Goedken, *J. Am. Chem. Soc.*, **95**, 3869 (1973).
(29) M. C. Weiss and V. L. Goedken, *J. Am. Chem. Soc.*, **98**, 3389 (1976).
(30) V. L. Goedken and S.-M. Peng, *J. Am. Chem. Soc.*, **96**, 7826 (1975).
(31) B. C. Chow and I. A. Cohen, *Bioinorg. Chem.*, **1**, 57 (1971).
(32) M. Tsutsui, D. Ostfeld, J. N. Francis, and L. M. Hoffman, *J. Am. Chem. Soc.*, **93**, 820 (1971).
(33) M. Tsutsui, D. Ostfeld, J. N. Francis, and L. M. Hoffman, *J. Coord. Chem.*, **1**, 115 (1971).
(34) S. S. Eaton, G. R. Eaton, and R. H. Holm, *J. Organomet. Chem.*, **32**, C52 (1971).
(35) S. S. Eaton, G. R. Eaton, and R. H. Holm, *J. Organomet. Chem.*, **39**, 179 (1972).
(36) J. W. Buchler, K. Lam Lay, P. D. Smith, W. R. Scheidt, G. A. Rupprecht, and J. E. Kenny, *J. Organomet. Chem.*, **110**, 109 (1976).
(37) G. R. Eaton and S. S. Eaton, *J. Am. Chem. Soc.*, **97**, 235 (1975).
(38) J. J. Bonnet, S. S. Eaton, G. R. Eaton, R. H. Holm, and J. A. Ibers, *J. Am. Chem. Soc.*, **95**, 2141 (1973).
(39) R. G. Little and J. A. Ibers, *J. Am. Chem. Soc.*, **95**, 8583 (1973).
(40) J. L. Hoard, *Science*, **174**, 1295 (1971), and references cited therein.
(41) D. M. Collins, R. Countryman, and J. L. Hoard, *J. Am. Chem. Soc.*, **94**, 2066 (1972).
(42) L. J. Radonovich, A. Bloom, and J. L. Hoard, *J. Am. Chem. Soc.*, **94**, 2072 (1972).
(43) J. P. Collman, J. L. Hoard, N. Kim, G. Long, and C. A. Reed, *J. Am. Chem. Soc.*, **97**, 2676 (1975).